Altered Global and Regional Brain Mean Diffusivity in Patients With Obstructive Sleep Apnea

Rajesh Kumar,[1] Alexa S. Chavez,[1] Paul M. Macey,[2,3] Mary A. Woo,[2] Frisca L. Yan-Go,[4] and Ronald M. Harper[1,3]★

[1]Department of Neurobiology, David Geffen School of Medicine at UCLA, University of California at Los Angeles, Los Angeles, California
[2]UCLA School of Nursing, University of California at Los Angeles, Los Angeles, California
[3]Brain Research Institute, University of California at Los Angeles, Los Angeles, California
[4]Department of Neurology, David Geffen School of Medicine at UCLA, University of California at Los Angeles, Los Angeles, California

Obstructive sleep apnea (OSA) is a common and progressive disorder accompanied by severe cardiovascular and neuropsychological sequelae, presumably induced by brain injury resulting from the intermittent hypoxia and cardiovascular processes accompanying the syndrome. However, whether the predominant brain tissue pathology is acute or chronic in newly-diagnosed, untreated OSA subjects is unclear; this assessment is essential for revealing pathological processes. Diffusion tensor imaging (DTI)-based mean diffusivity (MD) procedures can detect and differentiate acute from chronic pathology and may be useful to reveal processes in the condition. We collected four DTI series from 23 newly-diagnosed, treatment-naïve OSA and 23 control subjects, using a 3.0-Tesla magnetic resonance imaging scanner. Mean diffusivity maps were calculated from each series, realigned, averaged, normalized to a common space, and smoothed. Global brain MD values for each subject were calculated using normalized MD maps and a global brain mask. Mean global brain MD values and smoothed MD maps were compared between groups by using analysis of covariance (covariate: age). Mean global brain MD values were significantly reduced in OSA compared with controls ($P = 0.01$). Multiple brain sites in OSA, including medullary, cerebellar, basal ganglia, prefrontal and frontal, limbic, insular, cingulum bundle, external capsule, corpus callosum, temporal, occipital, and corona radiata regions showed reduced regional MD values compared with controls. The results suggest that global brain MD values are significantly reduced in OSA, with certain regional sites especially affected, presumably a consequence of axonal, glial, and other cell changes in those areas. The findings likely represent acute pathological processes in newly-diagnosed OSA subjects. © 2012 Wiley Periodicals, Inc.

Key words: diffusion tensor imaging; acute condition; cytotoxic edema; vasogenic edema; sleep-disordered breathing

Obstructive sleep apnea (OSA) is a common and progressive condition associated with serious comorbidities (Peppard et al., 2000; Elmasry et al., 2001; Shahar et al., 2001; Gami et al., 2004; Punjabi et al., 2004; Arzt et al., 2005; Bradley and Floras, 2009), and affects about 10% of the adult population in the United States (Young et al., 2002; Lee et al., 2008). Significant brain injury accompanies the syndrome, principally in cerebellar and limbic regions and interconnecting fibers, as well as limbic cortex (Macey et al., 2002, 2008; Cross et al., 2008; Kumar et al., 2009; Yaouhi et al., 2009; Zhang et al., 2009; Joo et al., 2010; Morrell et al., 2010). The injury likely contributes to the exaggerated sympathetic tone and high incidence of hypertension and cardiac arrhythmia (Peppard et al., 2000), as well as short-term memory and planning deficits, and increased mood and anxiety symptoms found in the condition (Naegele et al., 1998; Ferini-Strambi et al., 2003; Felver-Gant et al., 2007; Lis et al., 2008; Saunamaki et al., 2009, 2010). However, it is unclear whether the predominant pathology is acute or chronic in newly-diagnosed OSA subjects. Determining the pathological nature of injury in those subjects is essential, because it is unknown, for example, whether the principal "gold standard" for OSA intervention, continuous positive airway pressure, can recover brain tissue from chronic damage, or whether other interventions must be considered, even for acute brain changes in OSA patients. Such descriptions of injury nature will

assist in interpretation of the processes contributing to tissue damage.

Diffusion tensor imaging (DTI)-based fractional anisotropy (FA) and mean diffusivity (MD) procedures are commonly-used measures to examine tissue changes (Basser and Pierpaoli, 1998; Le Bihan et al., 2001). FA measures tissue organization, and can detect pathological tissue (Basser and Pierpaoli, 1996); the procedures do not differentiate the stage of tissue injury (Neil et al., 1998; Basser and Jones, 2002; Beaulieu, 2002). Axonal loss and demyelination are reflected by decreased FA values in chronic stages of tissue injury (Trip et al., 2006; Li et al., 2011), and both acute (Ward et al., 2006; Shereen et al., 2011) and subacute (between acute and chronic) stages after hypoxia are also associated with reduced FA values (Ward et al., 2006). However, MD procedures distinguish acute from chronic stages after hypoxia/ischemia, with decreased values in acute stages, values similar to those of normal conditions in subacute stages, and increased values in chronic stages (Matsumoto et al., 1995; Ahlhelm et al., 2002). Thus, MD procedures are more sensitive than FA in differentiating pathological stages, and may be useful in determining the pathological nature of brain injury in OSA subjects.

Our aim was to assess global mean and regional brain MD values in newly-diagnosed, treatment-naïve OSA over age- and gender-matched control subjects using DTI procedures. We hypothesized that global mean MD values will be reduced in OSA patients compared with control subjects, and localized declines in MD values will appear in multiple brain areas, indicative of acute injury at those sites.

MATERIALS AND METHODS

Subjects

We studied 23 OSA subjects (age 44.4 ± 9.3 years, body mass index [BMI] 30.1 ± 5.4 kg/m^2, apnea hypopnea index 34.9 ± 24.1 events/hr, 20 males) and 23 age- and gender-matched control subjects (age 45.3 ± 11.0 years, BMI 26.2 ± 3.7 kg/m^2, 20 males). These subjects were part of a large study, and OSA and control subjects included here were selected to match for similar age range, gender, and exact magnetic resonance imaging (MRI) scanning parameters, resulting in 23 OSA and 23 control subjects. All OSA subjects were newly-diagnosed via overnight polysomnography with at least moderate severity (apnea hypopnea index ≥ 15), treatment-naïve for breathing condition, and recruited from an accredited sleep-disorders laboratory at the University of California at Los Angeles (UCLA) Medical Center. No OSA subjects were taking any cardiovascular-altering medications, such as β-blockers, α-agonists, angiotensin-converting enzyme inhibitors, or vasodilators, or mood altering drugs, such as serotonin reuptake inhibitors. Subjects were also without any history of stroke, heart failure, diagnosed brain conditions, metallic implants, or body weight more than 125 kg (the last issue was a scanner limitation). All control subjects were interviewed, with their cosleeper when possible, to rule out any undetermined OSA condition; subjects were referred for an overnight polysomnography if such a condition was suspected. Control subjects were without any medications that might alter brain tissue, with no contradictions to the MRI scanner environment, and were recruited from the UCLA campus and West Los Angeles area. All procedures were carried out in accordance with the Declaration of Helsinki and approved by the Institutional Review Board at UCLA, and subjects provided written informed consent prior to the study.

MRI

Brain imaging studies were performed using a 3.0-Tesla MRI scanner (Magnetom Tim-Trio, Siemens, Erlangen, Germany), with a receive-only eight-channel phased-array head coil and a whole-body transmitter coil. We placed foam pads on both sides of the head to minimize head motion. High-resolution T1-weighted images were acquired using a magnetization-prepared rapid-acquisition-gradient echo pulse sequence (repetition time [TR] = 2,200 msec, echo time [TE] = 2.2 msec, inversion time = 900 msec, flip angle = 9°, matrix size = 256 × 256, field of view [FOV] = 230 × 230 mm, slice thickness = 1.0 mm). Proton density (PD) and T2-weighted images were collected simultaneously in the axial plane, using a dual-echo turbo spin-echo pulse sequence (TR = 10,000 msec, TE1 and 2 = 17 and 134 msec, flip angle = 130°, matrix size = 256 × 256, FOV = 230 × 230 mm, slice thickness = 4.0 mm). DTI data were acquired using single-shot echo-planar imaging with twice-refocused spin-echo pulse sequence (TR = 10,000 msec, TE = 87 msec, flip angle = 90°, bandwidth = 1,346 Hz/pixel, matrix size = 128 × 128, FOV = 230 × 230 mm, slice thickness = 2.0 mm, b = 0 and 700 sec/mm^2, diffusion directions = 12). We collected four separate DTI series with the same imaging protocol for subsequent averaging. We used the parallel imaging technique, generalized autocalibrating partially parallel acquisition, with an acceleration factor of two in all MRI data acquisition.

Data Processing and Analysis

The statistical parametric mapping package SPM8 (http://www.fil.ion.ucl.ac.uk/spm/), DTI-Studio 3.0.1 (Jiang et al., 2006), MRIcroN (Rorden et al., 2007), and MATLAB-based (http://www.mathworks.com/) custom-written software were used for data processing and analyses. We used high-resolution T1-, PD-, and T2-weighted images of OSA and control subjects to examine for any visible brain tissue pathology such as tumors, cysts, or any other major mass lesion. Diffusion- and nondiffusion-weighted images of all OSA and control subjects were also assessed for any head-motion-related or other imaging artifacts before MD calculation. No subjects (OSA or controls) included in this study showed any major visible brain pathology, head motion, or other imaging artifacts.

MD calculation. We calculated the average background noise level from outside the brain parenchyma by using nondiffusion- and diffusion-weighted images, and this noise threshold was used in all OSA and control subjects to suppress nonbrain regions (only those regions outside the brain parenchyma) during MD calculations. We used diffusion

(b = 700 sec/mm^2)-weighted images, collected from 12 diffusion directions, and nondiffusion (b = 0 sec/mm^2)-weighted images to compute diffusion tensor matrices in DTI-Studio software (Jiang et al., 2006). The diffusion tensor matrices were diagonalized, and principal eigenvalues (λ1, λ2, and λ3) were calculated (Pierpaoli et al., 1996; Basser and Pierpaoli, 1998). Using these principal eigenvalues, MD values [(λ1 + λ2 + λ3)/3] were calculated at each voxel (Pierpaoli et al., 1996; Le Bihan et al., 2001), with voxel intensities on the MD maps representing the corresponding MD values.

Realignment, averaging, normalization, and smoothing of MD maps. We realigned the four MD maps, computed from each DTI series, to remove any potential differences in alignment resulting from head–motion, and averaged to create one MD map per subject. Nondiffusion-weighted images (b0 images) were also realigned and averaged.

The averaged MD maps were normalized to Montreal Neurological Institute (MNI) space. For normalization of MD maps, averaged nondiffusion-weighted images were normalized to MNI space, based on *a priori*-defined distributions of gray matter, white matter, and cerebrospinal fluid tissue types (Ashburner and Friston, 2005), and the resulting normalization parameters were applied to corresponding MD maps and nondiffusion-weighted images. The normalized MD maps were smoothed with an isotropic Gaussian filter (10 mm kernel). High-resolution T1-weighted images of OSA and control subjects were also normalized to MNI space. T1-weighted images were partitioned into gray matter, white matter, and cerebrospinal fluid tissue types, based on a unified segmentation approach (Ashburner and Friston, 2005), and normalization parameters were applied to corresponding T1-weighted images. The normalized images of all OSA and control subjects were averaged to create a whole-brain mean image (background image), which was used for structural identification.

Global brain mask. The normalized white matter probability maps from OSA and control subjects were averaged, and similarly, gray matter probability maps from all subjects were averaged. The averaged gray and white matter probability maps were thresholded (white matter probability > 0.3, gray matter probability > 0.3) and combined to create a global brain mask.

Calculation of global brain MD values. Using a global brain mask, the normalized MD maps of all OSA and control individuals were masked to remove cerebrospinal fluid and other nonbrain regions. The masked MD maps were used to calculate mean global brain MD values with MATLAB-based custom-written software.

Statistical Analysis

The Statistical Package for the Social Sciences 18.0 (SPSS, Chicago, IL) was used to assess demographic and mean global brain MD data. We used independent-samples t-tests and χ^2 to examine the demographic data. The mean global brain MD values were assessed for significant differences between groups using analysis of covariance (ANCOVA), with age included as covariate. Significance levels were set at $P < 0.05$ for all the statistical tests.

We compared the normalized and smoothed MD maps voxel-by-voxel between OSA and control groups using ANCOVA, with age as covariate (SPM8, uncorrected threshold, $P < 0.005$; minimum extended cluster size five voxels). The extended cluster size was arbitrary and was used to avoid brain sites showing significant differences between groups with a cluster size fewer than five voxels, which may not represent reliable findings (Kumar et al., 2011). The brain clusters with significant differences between OSA and control groups were overlaid onto background image for structural identification.

Region-of-Interest Analyses

We also performed region-of-interest (ROI) analyses to determine average MD values in those areas that show significant differences between OSA and control subjects based on whole-brain voxel-by-voxel comparisons. ROI masks were outlined for various brain areas with clusters determined by voxel-by-voxel analysis procedures, and used to calculate average MD values of those sites from individual OSA and control subjects by using normalized and smoothed MD maps. The average MD values of those areas were compared between groups with multivariate ANCOVA (covariate, age) in SPSS software.

RESULTS

Demographics

No significant differences in age ($P = 0.77$) or gender ($P = 1.0$) appeared between the groups. However, BMI showed significant group differences ($P = 0.007$); OSA subjects had significantly increased BMI over controls.

Global MD Changes

The mean global brain MD value in control subjects was $1.045 \pm 0.072 \times 10^{-3}$ mm^2/sec, and in OSA subjects was $1.003 \pm 0.062 \times 10^{-3}$ mm^2/sec. The mean global brain MD value was significantly reduced in OSA compared with control subjects ($P = 0.012$).

Regional Voxel-by-Voxel MD Changes

Multiple brain areas in OSA subjects showed reduced MD values compared with control subjects, with age-related changes controlled. No brain sites showed increased MD values in OSA over control subjects. Brain sites in OSA that showed reduced MD values included the dorsal (Fig. 1a), ventral (Fig. 1e), and ventrolateral (Fig. 1f) medulla, left cerebellar uvula (Fig. 1b), bilateral cerebellar crus I (Fig. 1c), right cerebellar crus II, extending to the middle cerebellar peduncle (Fig. 1g), right medial/inferior cerebellar peduncle (Fig. 1d), left ventrolateral temporal lobe (Fig. 1h), bilateral dorsal temporal white matter extending to the occipital cortex (Fig. 1i), left ventral (Fig. 1k) and right middle (Fig. 1n) hippocampus, bilateral putamen (Fig. 1j), right insular cortex (Fig. 1m), bilateral posterior thalamus (Fig. 2a), left anterior thalamus (Fig. 2c), left caudal external capsule (Fig. 2b), anterior corpus callosum (Fig. 2d), bilateral frontal (Fig. 2e) and occipital (Fig. 2f) white matter; left prefrontal cortex (Fig. 2g), right middle and
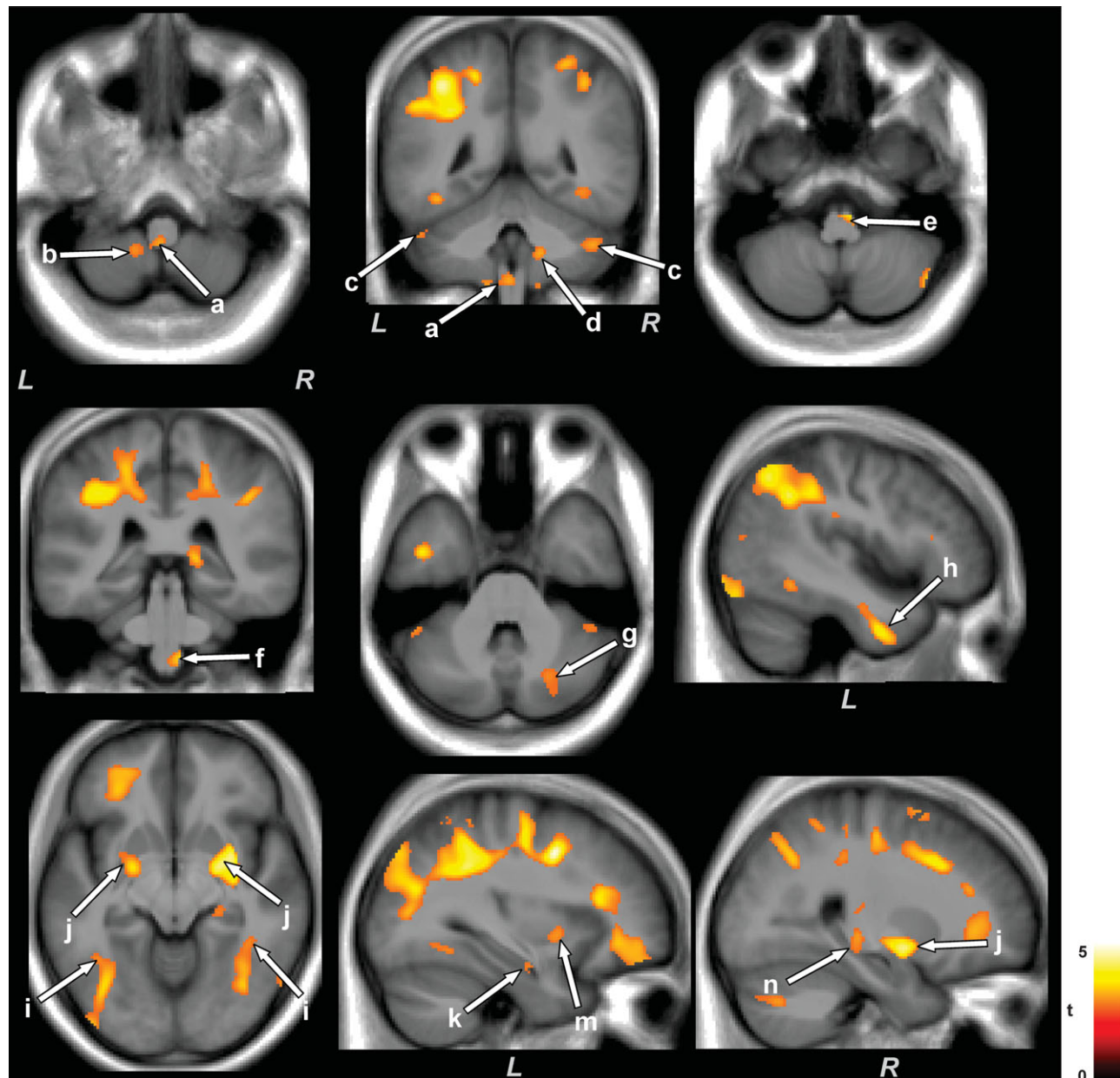
Fig. 1. Medullary, cerebellar, temporal, basal ganglia, and limbic brain areas with reduced MD values in OSA compared with control subjects. Multiple brain areas, including the dorsal (a), ventral (e), and ventrolateral (f) medulla, cerebellar uvula (b), cerebellar crus I and II (c,g), middle and inferior cerebellar peduncles (d), ventrolateral temporal lobe (h), dorsal temporal white matter and occipital cortex (i), ventral (k) and middle (n) hippocampus, putamen (j), and insular cortex (m), showed reduced MD values in OSA compared with control subjects. All brain images are shown with neurological conventions, with the left side of the brain on left side of the axial and coronal images (L, left; R, right), and the color bar represents t values.

posterior cingulate and cingulum bundle (Fig. 2h,i), and bilateral anterior (Fig. 2j), middle (Fig. 2k), and posterior (Fig. 2m) corona radiata.

ROI Analyses

The regional MD values calculated from various brain sites from OSA and control groups are summarized in Table I. Significantly reduced MD values emerged in all brain regions in OSA compared with control subjects, consistent with whole-brain voxel-based analysis findings.

DISCUSSION

Newly-diagnosed, treatment-naïve OSA subjects showed significantly reduced global brain MD values, and these changes were localized in various brain regions including medullary and brainstem areas critical for
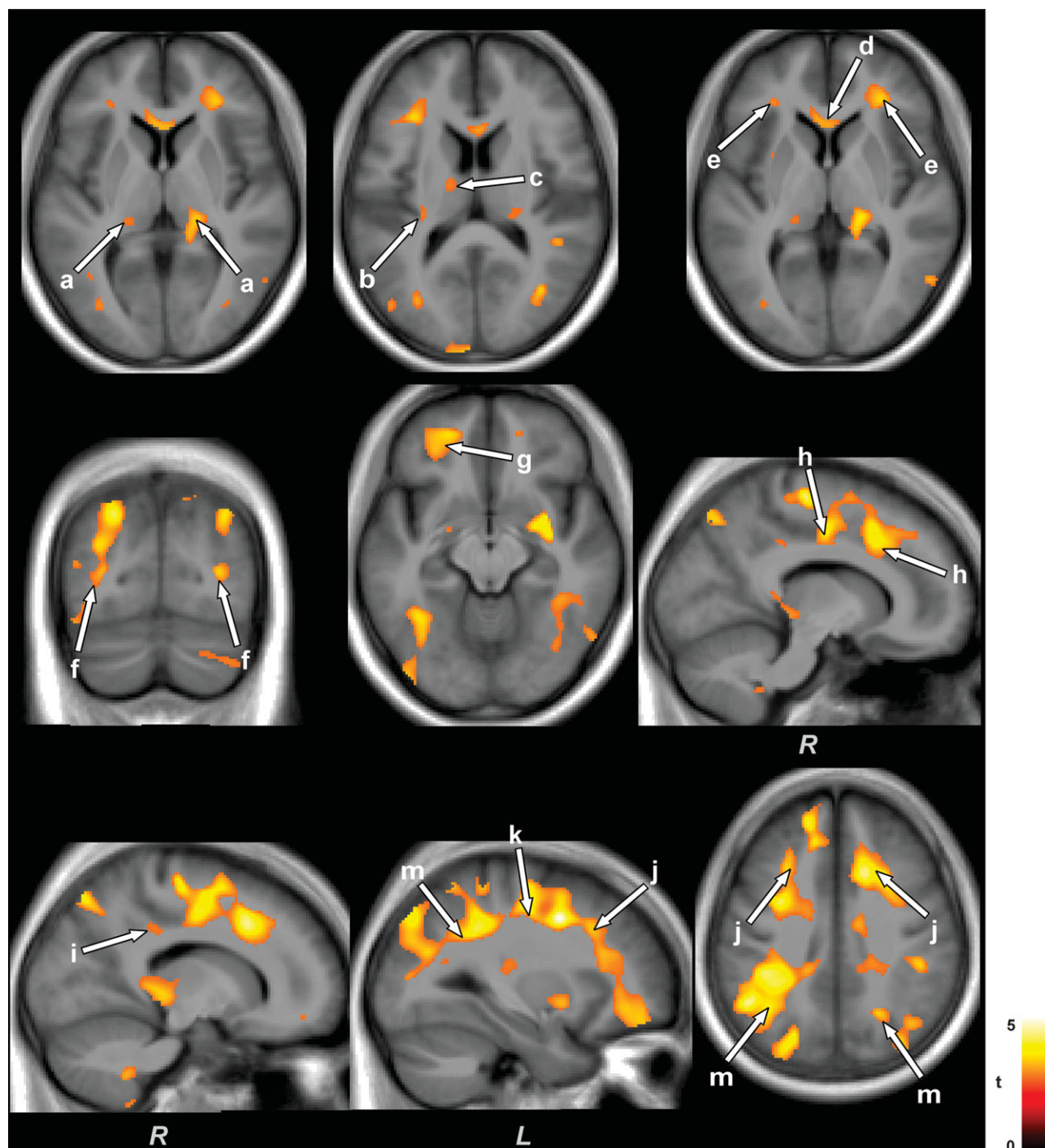
Fig. 2. Thalamic, corpus callosum, frontal, occipital, cingulate, and corona radiata regions with decreased MD values in OSA compared with control subjects. Brain regions with decreased MD values in OSA emerged in thalamic areas (a,c), external capsule (b), anterior corpus callosum (d), frontal (e) and occipital (f) white matter, prefrontal cortex (g), middle and posterior cingulate cortices and cingulum bundle (h,i), and anterior (j), middle (k), and posterior (m) corona radiata. Figure conventions are the same as in Figure 1.

cardiovascular and respiratory regulation, cerebellar, basal ganglia, hippocampal and other limbic sites, and the corona radiata. The nature of MD changes in OSA (decreased values) indicates that the alterations are from a predominantly acute stage.

OSA and Brain Injury

Regional gray matter volume loss and fiber injury as well as brain metabolic abnormalities appear in multiple brain areas in OSA subjects. Gray matter tissue loss appears in the cingulate and insular cortices, mammillary

TABLE I. Regional Brain Mean Diffusivity ($\times 10^{-3}$ mm^2/sec) Differences Between OSA* and Control Subjects

Brain site	OSA (n = 23) mean diffusivity (A)	Controls (n = 23) mean diffusivity (B)	P values, A vs. B
Ventral medulla	2.00 ± 0.22	2.18 ± 0.15	0.002
Ventrolateral medulla	2.02 ± 0.22	2.19 ± 0.15	0.003
L cerebellar uvula	1.59 ± 0.23	1.79 ± 0.18	0.003
L cerebellar crus I	1.37 ± 0.24	1.57 ± 0.30	0.007
R cerebellar crus I	1.23 ± 0.16	1.40 ± 0.25	0.004
R middle cerebellar peduncle	0.80 ± 0.05	0.86 ± 0.09	0.002
R medial inferior cerebellar peduncle	1.00 ± 0.09	1.08 ± 0.07	0.003
L ventrolateral temporal lobe	0.89 ± 0.05	0.95 ± 0.05	<0.001
L dorsal temporal white matter	0.81 ± 0.04	0.85 ± 0.04	<0.001
R dorsal temporal white matter	0.80 ± 0.04	0.84 ± 0.04	0.001
L ventral hippocampus	1.05 ± 0.06	1.13 ± 0.12	0.006
R midhippocampus	0.99 ± 0.08	1.07 ± 0.10	0.003
L putamen	0.84 ± 0.04	0.88 ± 0.04	0.001
R putamen	0.87 ± 0.03	0.92 ± 0.05	<0.001
L insular cortex	0.85 ± 0.03	0.88 ± 0.04	0.002
R insular cortex	0.89 ± 0.03	0.93 ± 0.06	<0.001
L posterior thalamus	0.91 ± 0.10	1.00 ± 0.10	0.008
R posterior thalamus	1.11 ± 0.10	1.21 ± 0.11	0.002
L anterior thalamus	1.18 ± 0.14	1.31 ± 0.19	0.007
L caudal external capsule	0.87 ± 0.05	0.92 ± 0.06	0.007
Anterior corpus callosum	1.45 ± 0.13	1.59 ± 0.16	0.003
L frontal white matter	0.86 ± 0.04	0.90 ± 0.06	0.006
R frontal white matter	0.83 ± 0.03	0.86 ± 0.05	0.003
L occipital white matter	0.80 ± 0.03	0.83 ± 0.04	0.003
R occipital white matter	0.82 ± 0.02	0.85 ± 0.04	0.002
L prefrontal cortex	0.95 ± 0.05	1.02 ± 0.10	0.001
R midcingulate	0.88 ± 0.04	0.94 ± 0.09	<0.001
R posterior cingulate	0.93 ± 0.05	0.97 ± 0.05	0.005
L anterior corona radiata	0.81 ± 0.03	0.86 ± 0.06	<0.001
R anterior corona radiata	0.82 ± 0.03	0.87 ± 0.06	<0.001
L midcorona radiata	0.95 ± 0.05	1.04 ± 0.09	<0.001
R midcorona radiata	0.93 ± 0.04	1.00 ± 0.07	<0.001
L posterior corona radiata	1.00 ± 0.11	1.12 ± 0.12	<0.001
R posterior corona radiata	1.12 ± 0.11	1.27 ± 0.17	0.001

*OSA, obstructive sleep apnea; L, left; R, right.

bodies, hippocampus, caudate and thalamus, cerebellar areas, and frontal, parietal, and temporal regions (Macey et al., 2002; Kumar et al., 2008; Yaouhi et al., 2009; Joo et al., 2010), and metabolic abnormalities emerge in the hippocampus, parietal-occipital cortex, centrum semiovale, and frontal and midtemporal areas (Kamba et al., 2003; Morrell et al., 2003; Tonon et al., 2007; Sarchielli et al., 2008). Fiber changes in newly-diagnosed OSA subjects, assessed by DTI-based FA procedures, appear in the corpus callosum, cingulum bundle, fornix, internal capsule, cerebellum and peduncles, and corticospinal tract (Macey et al., 2008; Zhang et al., 2009). These brain areas with FA changes are similar to those found here with MD procedures, although MD changes are more widespread than FA changes. The current study addresses the issue of whether OSA subjects show acute tissue changes from initial detection of the syndrome, or whether chronic injury appears at that time. Metabolic abnormalities and fiber changes, assessed with MR spectroscopy and FA procedures, can appear in early as well as chronic stages of tissue changes, and gray matter volume losses indicate chronic pathological changes. However, earlier studies might have had variations between scanning evaluation and time of diagnosis in OSA subjects (Macey et al., 2002; Joo et al., 2010; Morrell et al., 2010), possibly leading to discrepancies between MD and gray matter findings, since increased MD values would be expected in those sites with gray matter volume loss. The findings from MD procedures provide insights into those issues.

Reduced MD Values and Source of Tissue Injury

The injury characteristics provide clues to the source of injury; the MD changes are heavily lateralized, suggesting consequences of perfusion, oxygenation, or reperfusion from the normally asymmetrical vascular supply to the brain to the intermittent hypoxia aspects of OSA (Joo et al., 2007), affecting both glia and neurons. Neurons in certain structures are especially vulnerable from excitotoxic processes during intermittent hypoxia or impaired perfusion in OSA. These areas include hippocampal CA1 regions, cerebellar Purkinje cells, the anterior cingulate, and the mammillary bodies, sites that are recipients of long-projecting axons from Schaeffer's collaterals, inferior olive climbing fibers, cingulum bundle, and fornix, respectively (Shibata, 1992; Welsh et al., 2002; Aggleton et al., 2005; Ang et al., 2006); the targeted structures show lower MD values. Thus, we speculate that the lateralized regional brain damage develops from preferential vascular lateralization, which is compromised in OSA through the extreme cardiovascular changes accompanying each apneic event leading to ischemia. In addition, hypoxia from apnea events leads to excessive neural discharge and excitotoxic injury. Frontal, cerebellar, medullary, and other limbic areas show tissue injury in animal studies to intermittent hypoxic exposure, following protocols attempting to simulate OSA (Gozal et al., 2001; Veasey et al., 2004; Pae et al., 2005; Zhang et al., 2010).

Patients with stroke resulting from transient ischemia with acute diffusion changes show tissue and function recovery, if the ischemic condition is reversed quickly and forcefully (Kidwell et al., 1999; Lecouvet et al., 1999). As in stroke treatment strategies, acute tissue changes in newly-diagnosed OSA subjects suggest a possibility for recovery of abnormal tissue and function with use of anti-inflammatory and myelin-repair agents, together with aggressive intervention for the breathing condition.

Effect of Hypoxemia on Brain Tissue

Hypoxia and ischemia both decrease O_2 supply to brain tissue. During acute cerebral hypoxemia, as a result

of a mismatch between O_2 demand and supply, the failure of energy delivery results in cell depolarization, which modifies sodium and calcium ion movement into the cell, and potassium ions into extracellular space (Lowry et al., 1964; Hossmann, 1971; O'Dell et al., 1994; Dirnagl et al., 1999). Such ionic changes osmotically obligate water movement from extracellular to intracellular space, causing cell swelling (Mintorovitch et al., 1994), which in extreme hypoxia, results in cytotoxic edema. Excessive glutamate, released during cell depolarization, is neurotoxic (Benveniste et al., 1984; Hagberg et al., 1985); additional injury can develop from calcium ion influx (Edwards et al., 1998). The affected neurons and glia cells, especially myelin-supporting oligodendrocytes cells, which play critical roles in maintaining axonal function and survival (Kassmann and Nave, 2008), and are highly susceptible to hypoxemia, can lead to myelin separation from axons along with myelin and axonal swelling (Nukada and Dyck, 1987; Shereen et al., 2011), with a decrease in the extracellular volume fraction. The increased cellular cytotoxic edema and intra-axonal water, reflected as reduced extracellular/extra-axonal volume and extra-axonal water, are readily detected with MD measures.

Cytotoxic edema can be accompanied by brain swelling, with consequent vascular compression, resulting in a reduction in cerebral perfusion and blood–brain barrier alterations (Baethmann, 2000; Xavier et al., 2003). The condition will allow water to leak from the vascular space into the extracellular/extra-axonal space, and thus, the subacute stage would be a mixture of cytotoxic and vasogenic edema (Xavier et al., 2003), i.e., cell/axonal swelling together with more water in extracellular/extra-axonal space (Matsumoto et al., 1995).

Since vasogenic edema itself works as an ischemic condition (Marmarou et al., 2000), more water in the extracellular/extra-axonal space in the subacute stage will accelerate tissue degenerative processes, leading to demyelination, axonal, and cell loss in chronic stages of hypoxemia (Matsumoto et al., 1995).

OSA subjects undergo intermittent hypoxia during sleep; some axons and cells may recover functions during waking, in a fashion similar to that in transient ischemia (Kidwell et al., 1999; Lecouvet et al., 1999). However, most axons and cells, depending on the severity of hypoxemia, may progress to a chronic pathological state over the long term. Animal studies simulating intermittent hypoxia in human conditions show apoptosis and injury in brain areas after as little as 5 hr of 12% O_2 intermittent exposure (Pae et al., 2005). Thus, OSA with repeated nocturnal apneic events likely leads to progressive pathological changes.

MD Changes in Different Stages of Pathology

MD of water within tissue is influenced by various factors, including tissue barriers (Le Bihan et al., 1991) and extracellular/extra-axonal fluid and space. In the case of acute stages of pathology after hypoxemia, cyto-toxic edematous actions decrease extracellular water and lead to cell and axonal swelling, reducing the extracellular space, resulting in restricted water diffusion and, thus, reduced MD values. Multiple studies with hypoxia/ischemia-induced injury in acute stages show reduced MD values (Matsumoto et al., 1995; Ahlhelm et al., 2002). Subacute stages of hypoxemia are accompanied by cytotoxic and vasogenic edema, along with axonal and myelin swelling. Cytotoxic edema reduces MD values as a consequence of increased tissue barriers, and vasogenic edema helps to increase MD values; thus, subacute stages of hypoxemia will show MD values either little-changed or similar to those of control conditions (Matsumoto et al., 1995; Ahlhelm et al., 2002). However, demyelination or axonal loss in chronic stages of hypoxemia will reduce tissue barriers, increase extracellular volume, and escalate vasogenic edema; all of these factors will contribute to increased MD values (Matsumoto et al., 1995; Ahlhelm et al., 2002).

Sites of Injury and Autonomic, Respiratory, and Neuropsychologic Deficits

A remarkable aspect of the MD findings was the specific sites of injury. Significant injury appeared in medullary sites, areas essential for regulation of blood pressure, chemosensation, and integration of baroreceptor and chemoreceptor afferents (Caverson et al., 1984; Stocker et al., 2007). Earlier studies did not use techniques that would address the issue of acute vs. chronic injury, and the very first studies of regional volume reduction in OSA (Macey et al., 2002) used procedures that could not adequately resolve volume changes in the small medulla. The MD procedures also found injury in numerous other autonomic areas, including the insular cortex, a major influence on hypothalamic regulation of both sympathetic and parasympathetic outflow (Zhang et al., 1999). In addition, portions of the cingulate cortex (Critchley et al., 2003) and ventromedial frontal cortex (King et al., 1999), which play significant roles in cardiovascular regulation, showed injury. Neurocognitive deficits associated with OSA depend on the hippocampus, putamen, cerebellum, and cingulate cortex, as well as integrity of the corpus callosum; all of those structures show injury as indicated by MD procedures. The findings support the long list of studies indicating neural changes that accompany the syndrome (Macey et al., 2002, 2008; Kamba et al., 2003; Morrell et al., 2003, 2010; Tonon et al., 2007; Sarchielli et al., 2008; Kumar et al., 2008; Yaouhi et al., 2009; Zhang et al., 2009; Joo et al., 2010), and additionally point to specific medullary areas that are affected in the syndrome.

Limitations

Limitations of this study include the unavailability of precise OSA disease durations in individual subjects and the absence of followup studies after respiratory support intervention. Although all OSA subjects were newly-diagnosed, OSA duration in these subjects may

be variable, depending on numerous issues that can delay recognition or assessment. However, since brain sites showed reduced MD values, indicating that the changes reflected an acute condition (Matsumoto et al., 1995; Ahlhelm et al., 2002), we believe that the greatest proportions of the subjects were in early stages of chronic neural changes. We have insufficient data from followup studies postbreathing intervention to support conclusions for reversibility of brain tissue damage and function in OSA. However, studies are in progress to answer these questions.

CONCLUSIONS

Mean global brain MD values are significantly reduced in newly-diagnosed, treatment-naïve OSA vs. control subjects, indicating an acute stage of tissue changes. These brain changes appeared regionally in critical cardiovascular and respiratory areas of the medulla, as well as in the cerebellum, basal ganglia, limbic regions, corpus callosum, and multiple regions in the corona radiata. The pathological mechanisms of tissue injury likely include ischemia- and hypoxia-induced processes, leading to acute tissue changes in the condition. The findings raise the possibility that the initial brain tissue injury and resulting impaired function in OSA subjects can be reversed to some extent, by adopting strategies analogous to those found useful in acute stroke treatment.

ACKNOWLEDGMENTS

REFERENCES

Aggleton JP, Vann SD, Saunders RC. 2005. Projections from the hippocampal region to the mammillary bodies in macaque monkeys. Eur J Neurosci 22:2519–2530.

Ahlhelm F, Schneider G, Backens M, Reith W, Hagen T. 2002. Time course of the apparent diffusion coefficient after cerebral infarction. Eur Radiol 12:2322–2329.

Ang CW, Carlson GC, Coulter DA. 2006. Massive and specific dysregulation of direct cortical input to the hippocampus in temporal lobe epilepsy. J Neurosci 26:11850–11856.

Arzt M, Young T, Finn L, Skatrud JB, Bradley TD. 2005. Association of sleep-disordered breathing and the occurrence of stroke. Am J Respir Crit Care Med 172:1447–1451.

Ashburner J, Friston KJ. 2005. Unified segmentation. NeuroImage 26:839–851.

Baethmann A. 2000. Brain edema and leukocyte–endothelial interactions in cerebral ischemia. In: Oehmichen M, editor. Brain hypoxia and ischemia. Research in legal medicine, vol 24. Lübeck, Germany: Schmidt-Römhild. p 85–99.

Basser PJ, Jones DK. 2002. Diffusion-tensor MRI: theory, experimental design and data analysis—a technical review. NMR Biomed 15:456–467.

Basser PJ, Pierpaoli C. 1996. Microstructural and physiological features of tissues elucidated by quantitative-diffusion-tensor MRI. J Magn Reson B 111:209–219.

Basser PJ, Pierpaoli C. 1998. A simplified method to measure the diffusion tensor from seven MR images. Magn Reson Med 39:928–934.

Beaulieu C. 2002. The basis of anisotropic water diffusion in the nervous system—a technical review. NMR Biomed 15:435–455.

Benveniste H, Drejer J, Schousboe A, Diemer NH. 1984. Elevation of the extracellular concentrations of glutamate and aspartate in rat hippocampus during transient cerebral ischemia monitored by intracerebral microdialysis. J Neurochem 43:1369–1374.

Bradley TD, Floras JS. 2009. Obstructive sleep apnoea and its cardiovascular consequences. Lancet 373:82–93.

Caverson MM, Ciriello J, Calaresu FR. 1984. Chemoreceptor and baroreceptor inputs to ventrolateral medullary neurons. Am J Physiol 247:R872–R879.

Critchley HD, Mathias CJ, Josephs O, O'Doherty J, Zanini S, Dewar BK, Cipolotti L, Shallice T, Dolan RJ. 2003. Human cingulate cortex and autonomic control: converging neuroimaging and clinical evidence. Brain 126:2139–2152.

Cross RL, Kumar R, Macey PM, Doering LV, Alger JR, Yan-Go FL, Harper RM. 2008. Neural alterations and depressive symptoms in obstructive sleep apnea patients. Sleep 31:1103–1109.

Dirnagl U, Iadecola C, Moskowitz MA. 1999. Pathobiology of ischaemic stroke: an integrated view. Trends Neurosci 22:391–397.

Edwards M, Kent TA, Rea HC, Wei J, Quast M, Izumi T, Mitra S, Perez-Polo JR. 1998. APE/Ref-1 responses to ischemia in rat brain. Neuroreport 9:4015–4018.

Elmasry A, Lindberg E, Berne C, Janson C, Gislason T, Awad Tageldin M, Boman G. 2001. Sleep-disordered breathing and glucose metabolism in hypertensive men: a population-based study. J Intern Med 249:153–161.

Felver-Gant JC, Bruce AS, Zimmerman M, Sweet LH, Millman RP, Aloia MS. 2007. Working memory in obstructive sleep apnea: construct validity and treatment effects. J Clin Sleep Med 3:589–594.

Ferini-Strambi L, Baietto C, Di Gioia MR, Castaldi P, Castronovo C, Zucconi M, Cappa SF. 2003. Cognitive dysfunction in patients with obstructive sleep apnea (OSA): partial reversibility after continuous positive airway pressure (CPAP). Brain Res Bull 61:87–92.

Gami AS, Pressman G, Caples SM, Kanagala R, Gard JJ, Davison DE, Malouf JF, Ammash NM, Friedman PA, Somers VK. 2004. Association of atrial fibrillation and obstructive sleep apnea. Circulation 110:364–367.

Gozal D, Daniel JM, Dohanich GP. 2001. Behavioral and anatomical correlates of chronic episodic hypoxia during sleep in the rat. J Neurosci 21:2442–2450.

Hagberg H, Lehmann A, Sandberg M, Nystrom B, Jacobson I, Hamberger A. 1985. Ischemia-induced shift of inhibitory and excitatory amino acids from intra- to extracellular compartments. J Cereb Blood Flow Metab 5:413–419.

Hossmann KA. 1971. Cortical steady potential, impedance and excitability changes during and after total ischemia of cat brain. Exp Neurol 32:163–175.

Jiang H, van Zijl PC, Kim J, Pearlson GD, Mori S. 2006. DtiStudio: resource program for diffusion tensor computation and fiber bundle tracking. Comput Methods Programs Biomed 81:106–116.

Joo EY, Tae WS, Han SJ, Cho JW, Hong SB. 2007. Reduced cerebral blood flow during wakefulness in obstructive sleep apnea-hypopnea syndrome. Sleep 30:1515–1520.

Joo EY, Tae WS, Lee MJ, Kang JW, Park HS, Lee JY, Suh M, Hong SB. 2010. Reduced brain gray matter concentration in patients with obstructive sleep apnea syndrome. Sleep 33:235–241.

Kamba M, Inoue Y, Higami S, Suto Y. 2003. Age-related changes in cerebral lactate metabolism in sleep-disordered breathing. Neurobiol Aging 24:753–760.

Kassmann CM, Nave KA. 2008. Oligodendroglial impact on axonal function and survival—a hypothesis. Curr Opin Neurol 21:235–241.

Kidwell CS, Alger JR, Di Salle F, Starkman S, Villablanca P, Bentson J, Saver JL. 1999. Diffusion MRI in patients with transient ischemic attacks. Stroke 30:1174–1180.

King AB, Menon RS, Hachinski V, Cechetto DF. 1999. Human forebrain activation by visceral stimuli. J Comp Neurol 413:572–582.

Kumar R, Birrer BV, Macey PM, Woo MA, Gupta RK, Yan-Go FL, Harper RM. 2008. Reduced mammillary body volume in patients with obstructive sleep apnea. Neurosci Lett 438:330–334.

Kumar R, Macey PM, Cross RL, Woo MA, Yan-Go FL, Harper RM. 2009. Neural alterations associated with anxiety symptoms in obstructive sleep apnea syndrome. Depress Anxiety 26:480–491.

Kumar R, Woo MA, Macey PM, Fonarow GC, Hamilton MA, Harper RM. 2011. Brain axonal and myelin evaluation in heart failure. J Neurol Sci 307:106–113.

Le Bihan D, Moonen CT, van Zijl PC, Pekar J, DesPres D. 1991. Measuring random microscopic motion of water in tissues with MR imaging: a cat brain study. J Comput Assist Tomogr 15:19–25.

Le Bihan D, Mangin JF, Poupon C, Clark CA, Pappata S, Molko N, Chabriat H. 2001. Diffusion tensor imaging: concepts and applications. J Magn Reson Imaging 13:534–546.

Lecouvet FE, Duprez TP, Raymackers JM, Peeters A, Cosnard G. 1999. Resolution of early diffusion-weighted and FLAIR MRI abnormalities in a patient with TIA. Neurology 52:1085–1087.

Lee W, Nagubadi S, Kryger MH, Mokhlesi B. 2008. Epidemiology of obstructive sleep apnea: a population-based perspective. Expert Rev Respir Med 2:349–364.

Li M, Li J, He H, Wang Z, Lv B, Li W, Hailla N, Yan F, Xian J, Ai L. 2011. Directional diffusivity changes in the optic nerve and optic radiation in optic neuritis. Br J Radiol 84:304–314.

Lis S, Krieger S, Hennig D, Roder C, Kirsch P, Seeger W, Gallhofer B, Schulz R. 2008. Executive functions and cognitive subprocesses in patients with obstructive sleep apnoea. J Sleep Res 17:271–280.

Lowry OH, Passonneau JV, Hasselberger FX, Schulz DW. 1964. Effect of ischemia on known substrates and cofactors of the glycolytic pathway in brain. J Biol Chem 239:18–30.

Macey PM, Henderson LA, Macey KE, Alger JR, Frysinger RC, Woo MA, Harper RK, Yan-Go FL, Harper RM. 2002. Brain morphology associated with obstructive sleep apnea. Am J Respir Crit Care Med 166:1382–1387.

Macey PM, Kumar R, Woo MA, Valladares EM, Yan-Go FL, Harper RM. 2008. Brain structural changes in obstructive sleep apnea. Sleep 31:967–977.

Marmarou A, Fatouros PP, Barzo P, Portella G, Yoshihara M, Tsuji O, Yamamoto T, Laine F, Signoretti S, Ward JD, Bullock MR, Young HF. 2000. Contribution of edema and cerebral blood volume to traumatic brain swelling in head-injured patients. J Neurosurg 93:183–193.

Matsumoto K, Lo EH, Pierce AR, Wei H, Garrido L, Kowall NW. 1995. Role of vasogenic edema and tissue cavitation in ischemic evolution on diffusion-weighted imaging: comparison with multiparameter MR and immunohistochemistry. Am J Neuroradiol 16:1107–1115.

Mintorovitch J, Yang GY, Shimizu H, Kucharczyk J, Chan PH, Weinstein PR. 1994. Diffusion-weighted magnetic resonance imaging of acute focal cerebral ischemia: comparison of signal intensity with changes in brain water and Na^+,K^+-ATPase activity. J Cereb Blood Flow Metab 14:332–336.

Morrell MJ, McRobbie DW, Quest RA, Cummin AR, Ghiassi R, Corfield DR. 2003. Changes in brain morphology associated with obstructive sleep apnea. Sleep Med 4:451–454.

Morrell MJ, Jackson ML, Twigg GL, Ghiassi R, McRobbie DW, Quest RA, Pardoe H, Pell GS, Abbott DF, Rochford PD, Jackson GD, Pierce RJ, O'Donoghue FJ, Corfield DR. 2010. Changes in brain morphology in patients with obstructive sleep apnoea. Thorax 65:908–914.

Naegele B, Pepin JL, Levy P, Bonnet C, Pellat J, Feuerstein C. 1998. Cognitive executive dysfunction in patients with obstructive sleep apnea syndrome (OSAS) after CPAP treatment. Sleep 21:392–397.

Neil JJ, Shiran SI, McKinstry RC, Schefft GL, Snyder AZ, Almli CR, Akbudak E, Aronovitz JA, Miller JP, Lee BC, Conturo TE. 1998. Normal brain in human newborns: apparent diffusion coefficient and diffusion anisotropy measured by using diffusion tensor MR imaging. Radiology 209:57–66.

Nukada H, Dyck PJ. 1987. Acute ischemia causes axonal stasis, swelling, attenuation, and secondary demyelination. Ann Neurol 22:311–318.

O'Dell TJ, Huang PL, Dawson TM, Dinerman JL, Snyder SH, Kandel ER, Fishman MC. 1994. Endothelial NOS and the blockade of LTP by NOS inhibitors in mice lacking neuronal NOS. Science 265:542–546.

Pae EK, Chien P, Harper RM. 2005. Intermittent hypoxia damages cerebellar cortex and deep nuclei. Neurosci Lett 375:123–128.

Peppard PE, Young T, Palta M, Skatrud J. 2000. Prospective study of the association between sleep-disordered breathing and hypertension. N Engl J Med 342:1378–1384.

Pierpaoli C, Jezzard P, Basser PJ, Barnett A, Di Chiro G. 1996. Diffusion tensor MR imaging of the human brain. Radiology 201:637–648.

Punjabi NM, Shahar E, Redline S, Gottlieb DJ, Givelber R, Resnick HE. 2004. Sleep-disordered breathing, glucose intolerance, and insulin resistance: the sleep heart health study. Am J Epidemiol 160:521–530.

Rorden C, Karnath HO, Bonilha L. 2007. Improving lesion-symptom mapping. J Cogn Neurosci 19:1081–1088.

Sarchielli P, Presciutti O, Alberti A, Tarducci R, Gobbi G, Galletti F, Costa C, Eusebi P, Calabresi P. 2008. A 1H magnetic resonance spectroscopy study in patients with obstructive sleep apnea. Eur J Neurol 15:1058–1064.

Saunamaki T, Himanen SL, Polo O, Jehkonen M. 2009. Executive dysfunction in patients with obstructive sleep apnea syndrome. Eur Neurol 62:237–242.

Saunamaki T, Himanen SL, Polo O, Jehkonen M. 2010. Executive dysfunction and learning effect after continuous positive airway pressure treatment in patients with obstructive sleep apnea syndrome. Eur Neurol 63:215–220.

Shahar E, Whitney CW, Redline S, Lee ET, Newman AB, Javier Nieto F, O'Connor GT, Boland LL, Schwartz JE, Samet JM. 2001. Sleep-disordered breathing and cardiovascular disease: cross-sectional results of the sleep heart health study. Am J Respir Crit Care Med 163:19–25.

Shereen A, Nemkul N, Yang D, Adhami F, Dunn RS, Hazen ML, Nakafuku M, Ning G, Lindquist DM, Kuan CY. 2011. Ex vivo diffusion tensor imaging and neuropathological correlation in a murine model of hypoxia-ischemia-induced thrombotic stroke. J Cereb Blood Flow Metab 31:1155–1169.

Shibata H. 1992. Topographic organization of subcortical projections to the anterior thalamic nuclei in the rat. J Comp Neurol 323:117–127.

Stocker SD, Meador R, Adams JM. 2007. Neurons of the rostral ventrolateral medulla contribute to obesity-induced hypertension in rats. Hypertension 49:640–646.

Tonon C, Vetrugno R, Lodi R, Gallassi R, Provini F, Iotti S, Plazzi G, Montagna P, Lugaresi E, Barbiroli B. 2007. Proton magnetic resonance spectroscopy study of brain metabolism in obstructive sleep apnoea syndrome before and after continuous positive airway pressure treatment. Sleep 30:305–311.

Trip SA, Wheeler-Kingshott C, Jones SJ, Li WY, Barker GJ, Thompson AJ, Plant GT, Miller DH. 2006. Optic nerve diffusion tensor imaging in optic neuritis. NeuroImage 30:498–505.

Veasey SC, Davis CW, Fenik P, Zhan G, Hsu YJ, Pratico D, Gow A. 2004. Long-term intermittent hypoxia in mice: protracted hypersomnolence with oxidative injury to sleep–wake brain regions. Sleep 27:194–201.

Ward P, Counsell S, Allsop J, Cowan F, Shen Y, Edwards D, Rutherford M. 2006. Reduced fractional anisotropy on diffusion tensor magnetic resonance imaging after hypoxic–ischemic encephalopathy. Pediatrics 117:e619–630.

Welsh JP, Yuen G, Placantonakis DG, Vu TQ, Haiss F, O'Hearn E, Molliver ME, Aicher SA. 2002. Why do Purkinje cells die so easily af-

ter global brain ischemia? Aldolase C, EAAT4, and the cerebellar contribution to posthypoxic myoclonus. Adv Neurol 89:331–359.

Xavier AR, Qureshi AI, Kirmani JF, Yahia AM, Bakshi R. 2003. Neuroimaging of stroke: a review. South Med J 96:367–379.

Yaouhi K, Bertran F, Clochon P, Mezenge F, Denise P, Foret J, Eustache F, Desgranges B. 2009. A combined neuropsychological and brain imaging study of obstructive sleep apnea. J Sleep Res 18:36–48.

Young T, Peppard PE, Gottlieb DJ. 2002. Epidemiology of obstructive sleep apnea: a population health perspective. Am J Respir Crit Care Med 165:1217–1239.

Zhang JH, Fung SJ, Xi M, Sampogna S, Chase MH. 2010. Apnea produces neuronal degeneration in the pons and medulla of guinea pigs. Neurobiol Dis 40:251–264.

Zhang XQ, Lu BX, Li TP. 2009. Correlation between white matter lesion and memory impairment in patients with obstructive sleep apnea syndrome. Nan Fang Yi Ke Da Xue Xue Bao 29:825–829.

Zhang ZH, Dougherty PM, Oppenheimer SM. 1999. Monkey insular cortex neurons respond to baroreceptive and somatosensory convergent inputs. Neuroscience 94:351–360.